Magnetic Resonance Imaging 63 (2019) 80–84

Contents lists available at ScienceDirect

Magnetic Resonance Imaging

journal homepage: www.elsevier.com/locate/mri

Original article

# Correlation of apparent diffusion coefficient and intravoxel incoherent motion imaging parameters with Ki-67 expression in extrahepatic cholangiocarcinoma

Xingyu Cui[a], Hongwei Chen[a,*], Song Cai[b], Qunfeng Tang[a], Xiangming Fang[a]

[a] Department of Radiology, Wuxi People's Hospital, Nanjing Medical University, Wuxi, Jiangsu Province, China
[b] Department of Radiology, Traditional Chinese Medicine Hospital of Wuxi City, Wuxi, Jiangsu Province, China

ARTICLE INFO

*Keywords:*
Extrahepatic cholangiocarcinoma
Diffusion-weighted imaging
Ki-67 antigen

ABSTRACT

*Purpose:* To investigate the correlation of magnetic resonance imaging (MRI), apparent diffusion coefficient (ADC) and intravoxel incoherent motion imaging parameters with Ki-67 expression in cholangiocarcinoma.

*Methods:* A total of 42 extrahepatic cholangiocarcinoma (EHCC) cases confirmed by surgical pathology were analyzed retrospectively. Subjects underwent MRI at 3.0 T and intravoxel incoherent motion diffusion-weighted imaging (IVIM-DWI) sequential scanning prior to surgery, and postoperative Ki-67 expression was recorded by immunohistochemistry (IHC). The patients were divided into 4 groups (I–IV) based on increasing Ki-67 expression from − to +++. ADC values and IVIM-DWI parameters were calculated, including true diffusion coefficient (D), perfusion fraction (f), and pseudo-diffusion coefficient (D*). The comparison among groups was analyzed by univariate ANOVA (normal distribution) or Kruskal-Wallis H (non-normal distribution). Spearman correlation analysis was used to analyze the correlation of each parameter with Ki-67 expression. The diagnostic efficiency of each parameter was compared using the area under the curve (AUC) of the receiver operating characteristic (ROC) curve.

*Results:* Except for D*, other values had statistically significant differences between groups ($P < 0.05$). ADC, D and f values had negative correlations with Ki-67 expression (r values were −0.607, −0.795, −0.531, respectively, $P < 0.05$). The AUCs were 0.701, 0.880, 0.623, respectively ($P < 0.0001$).

*Conclusion:* IVIM-DWI technology can reflect the proliferative activity of EHCC cells to a certain extent, and has clinical value for predicting the degree of malignancy of a tumor.

## 1. Introduction

Extrahepatic cholangiocarcinoma (EHCC), a malignant tumor derived from epithelial cells in the porta hepatis and extrahepatic bile duct, is characterized by rapid growth and poor prognosis [1]. Preoperative knowledge of its invasive potential is critical for appropriate surgical planning, and is also helpful to avoid overtreatment and improve quality of life [2,3]. The proliferative activity of tumor cells is one of the most reliable prognostic factors [4]. Ki-67 is a biological marker that can accurately reflect cell proliferation status [4]. Previous studies on MRI in breast cancer and rectal cancer have proven that the apparent diffusion coefficient (ADC) value on diffusion-weighted imaging (DWI) has a negative correlation with Ki-67 expression [5,6]. Recent meta-analysis studies [7–10] have also demonstrated that some tumors showed well inverse correlations between ADC and Ki-67 expression [11–13], and ADC can be used as an imaging marker for proliferation potential in this entity. In other tumors moderate correlations were identified between ADC and Ki-67 expression, and use of ADC as a surrogate marker for proliferation potential in clinical practice is limited [8]. However, DWI can only quantitatively analyze the diffusion motion of water molecules in tissues using a traditional single-index model, which is a limitation [14–16]. Intravoxel incoherent motion (IVIM) can evaluate diffusion in tissue and microvascular perfusion via more accurate quantitative parameters, and more clearly describes intravoxel micromotion [16]. In this study, we assessed for correlations of apparent diffusion coefficient (ADC) and IVIM-DWI parameters with Ki-67 expression, and explored the clinical value of IVIM-DWI determination of proliferative activity of EHCC cells prior to surgery.

* Corresponding author at: Department of Radiology, Wuxi People's Hospital, Nanjing Medical University, No.299, QingYang Rd, Wuxi 214023, Jiangsu Province, China.
*E-mail address:* chw6312@163.com (H. Chen).

https://doi.org/10.1016/j.mri.2019.08.018
Received 14 June 2019; Received in revised form 22 July 2019; Accepted 15 August 2019

## 2. Materials and methods

### 2.1. Clinical data

A total of 42 EHCC cases confirmed by surgical pathology from Jan. 2013 to Apr. 2018 were collected. Routine MRI scanning plus IVIM-DWI examinations were performed prior to surgery. Inclusion criteria: 1) EHCC confirmed by surgical pathology; 2) smallest size of lesion ≥1 cm; 3) complete information of each MRI sequence available and 4) image quality meeting the requirements for diagnosis. Twenty-two men and 20 women were enrolled. Age range was 29–83 y, and mean age was 64.03 ± 11.49 y. Main clinical manifestations included progressive obstructive jaundice, epigastric discomfort, and abdominal pain, sometimes associated with fever. Total bilirubin, direct bilirubin, and indirect bilirubin were elevated to different degrees, and 37 patients had elevated CA19-9.

### 2.2. Imaging examinations

A 3.0 T MRI scanner (Magnetom Trio Tim, SIEMENS, Erlangen, Germany) with a body phased-array coil were used. The patients were supine with the head in front. Before examination, the patients were fasted for 6–8 h, and received regular breathing and breath-hold training. The scanning range was from the diaphragmatic dome to the inferior border of the pancreas, including the complete biliary system. Conventional MRI scanning sequences included cross-sectional T1-weighted images (T1WI) with positive and negative phase gradient echo (GRE) sequences, a T2-weighted imaging (T2WI) turbo spin-echo (TSE) sequence, and a coronal T2WI half-Fourier acquisition single-shot-turbo-spin-echo(HASTE)sequence. Cross-sectional T1WI scanning parameters: TR 245 ms, TE 4.87/2.37 ms, FA 70°, FOV 350 × 396 mm, matrix 320 × 175 mm; T2WI scanning parameters: TR 3954 ms, TE 98 ms, FA 160°, FOV 350 × 396 mm, matrix 384 × 202 mm, thickness 5 mm, slice gap 1.5 mm; coronal T2WI scanning parameters: TR 1400 ms, TE 92 ms, FA 180°, FOV 400 × 450 mm, matrix 256 × 256 mm, thickness 5 mm, slice gap 1.5 mm.

Axial Spin echo-echo planar imaging (SE-EPI) sequences were used in IVIM-DWI. Diffusion sensitivity coefficients (b) were 0, 50, 100, 150, 200, 500, 800, 1000, and 1300 s/mm$^2$. Scanning parameters: TR 3510 ms, TE 79 ms, FA 90°, FOV 317 × 380 mm, matrix 168 × 10$^8$, thickness 5 mm, slice gap 1.5 mm. Total scanning time was 9 min.

### 2.3. Image analysis

Siemens IvimMain software was used to process the IVIM-DWI images. Two radiologists with > 10 y experience analyzed the data together. The DWI data with multiple b values were transmitted to IvimMain software, setting noise level as 20 and perfusion b < 200 to generate pseudo-color maps (b0, true diffusion coefficient [D], perfusion fraction [f], and pseudo-diffusion coefficient [D*]) representing diffusion information. MRI conventional sequence was used as a reference to observe the hepatic signal in IVIM images, as well as tumor size, morphology, boundaries, and extent. Cross-sectional T2WI at the same section level was used as a background reference, and regions of interest (ROIs) were placed on the maximum cross-sectional area of a lesion in the ADC image and the generated b0, D, f and D* images. The size and site of ROIs in different images from same patient were kept as close as possible. The measurement was performed in triplicate and averaged.

### 2.4. Pathological examination

All the EHCC immunohistochemical (IHC) sections were read by two physicians with > 5 y pathological diagnosis experience. Cells with pale brown granular deposits were considered to be Ki-67 positive. Ki-67 index is the percentage of positive cells in the densest visual field. The tumor lesions were divided into 4 groups according to the Ki-67 index: Group I, Ki-67 index < 10% (−); Group II, Ki-67 index 10%–25% (+); Group III, Ki-67 index 26%–50% (++); Group IV Ki-67 index > 50% (+++).

### 2.5. Statistics

Commercial software (SPSS 19.0, IBM Corporation, Armonk NY, USA) was used to analyze the data. Data meeting a normal distribution are expressed as mean ± SD, and non-normal data are expressed as median (M). Comparison between groups with different Ki-67 expression was tested by univariate ANOVA (normal distribution) or Kruskal-Wallis H (non-normal distribution). Spearman correlation analysis was used to analyze the correlation of each parameter with Ki-67 expression. Diagnostic efficiency was compared using ROC. The efficiency was rated low, moderate, or high, when AUC was 0.5–0.7, 0.7–0.9, and > 0.9, respectively. $P < 0.05$ was termed as statistically significant.

## 3. Results

### 3.1. IVIM-DWI and pathological manifestations of EHCC

The conventional MR sequences all indicated a mass or nodule in the bile duct. T1WI showed low or slightly low signal, and T2WI showed slightly high signal. Among them, 39 patients had relatively low signal in D value images (92.86%). In f value images, 25 EHCC patients had a significant difference in the signal intensity between the lesion and surrounding tissues (59.52%), 15 lesions were isointense, and 2 had slightly higher signal. Only 17 D* value images had significant differences in intensity between the lesion and the surrounding tissues (Fig. 1 A–F).

The 42 cases were confirmed as adenocarcinoma by surgical pathology. Ki-67 was expressed in most cells, showing uniform pale brown granules (Fig. 1 G–H).

Correlation of ADC and IVIM values with Ki-67 expression (Table 1).

The correlation coefficients of ADC, D, and f in EHCC with different Ki-67 expression levels were −0.607, −0.795, and −0.531, respectively ($P < 0.0001$), the values gradually decreasing with increasing Ki-67 expression levels. The correlations of ADC and D values with Ki-67 expression were more statistically significant than those of f values; those of D values showed the highest significance. D* value had no statistically significant difference with different Ki-67 expression ($P = 0.089$). AUCs of ADC, D, and f were 0.701, 0.880, and 0.623, respectively ($P < 0.0001$). The diagnostic accuracy of D was also the most significant.

## 4. Discussion

DWI is the only imaging method that can noninvasively detect microcosmic motion of water molecules in living bodies [14,15]. ADC values can be used to evaluate lesion infiltration degree, judge pathological grade, and identify benign and malignant lesions [14,15]. However, ADC calculated by a single-index model is influenced by water diffusion and microcirculation perfusion of blood capillaries, but it cannot reflect the real data of water diffusion in tissues. Le Bihan et al. [16] reported on the IVIM-DWI with multiple b values. According to double-index model fitting, diffusion and perfusion information of tissues was separated to obtain the D value that reflected true diffusion of water molecules. Meanwhile, D* and f were also obtained to reflect blood flow perfusion in a solid organ or lesion. As a sensitive biological marker monitoring proliferation, highly Ki-67 expression suggests active proliferation, vigorous growth, strong invasion, and poor prognosis [4]. Previous studies have proven that [17] ADC values in tumors are reduced with an elevated Ki-67 index. So far, IVIM-DWI and Ki-67 labeling indices have been applied in investigations of tumors of the

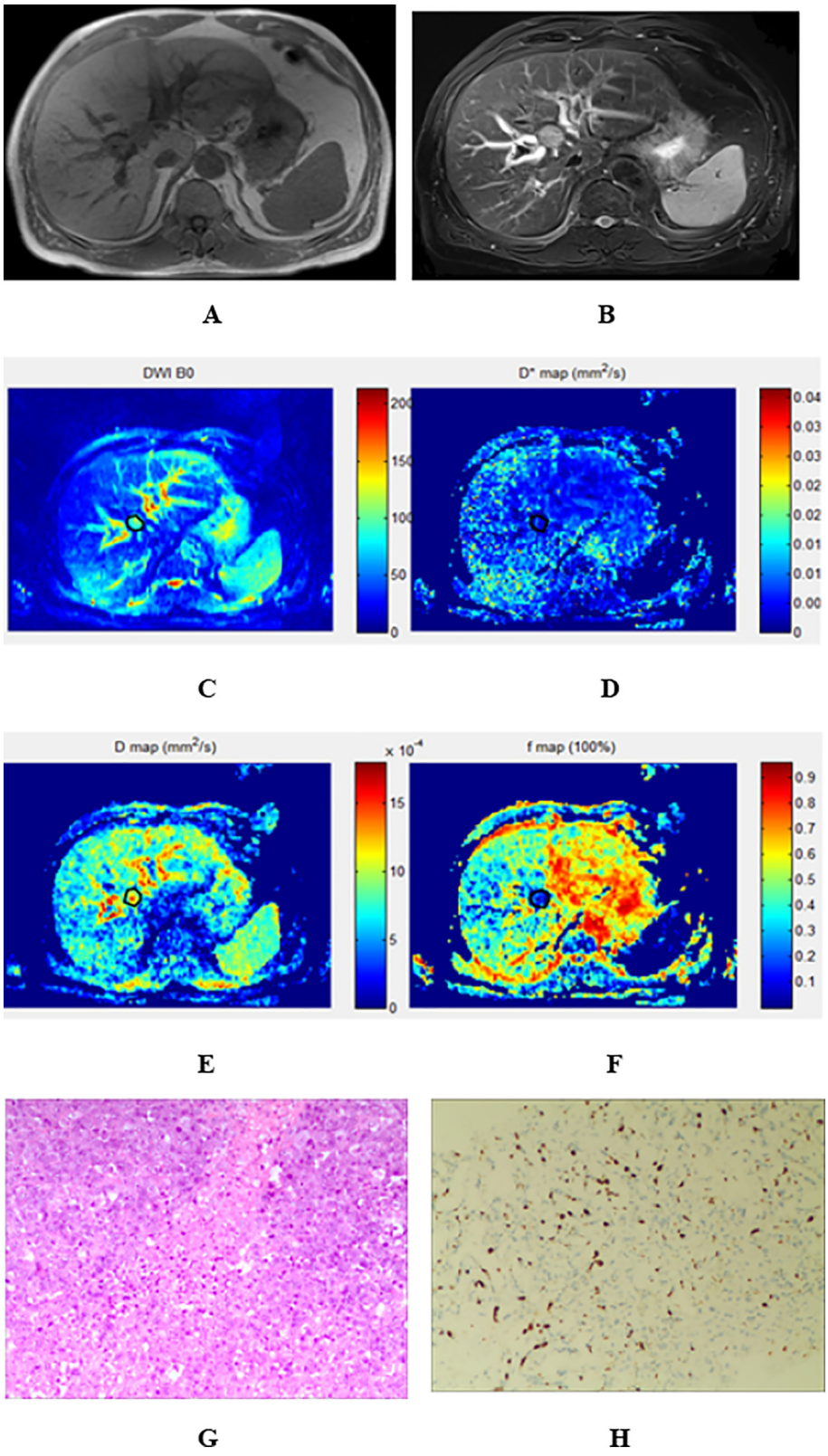


**Fig. 1.** Man, 67 years old, poorly differentiated hilar adenocarcinoma. A and B are MRI T1- and T2-weighted images, illustrating a 19 × 24 mm rounded soft tissue mass in the porta hepatis, with slightly long T1 and T2 signals, and a dilated intrahepatic bile duct. C–F are pseudo-color images of b0, D*, D and f, respectively, with ROI contoured in the lesion. b0, D, and *f* illustrate color staining in the lesion with nonuniform signal, distinguishable from surrounding normal liver parenchyma color, showing a clear boundary with surrounding tissues. D* illustrates shows no color contrast with surrounding tissues. G is a photomicrograph of poorly differentiated adenocarcinoma (H&E × 200). H shows uniform pale brown granules of Ki-67 (Ki-67 index is 35%) (immumohistochemical staining ×200). (For interpretation of the references to color in this figure legend, the reader is referred to the web version of this article.)

rectum, breast, and brain [6,18,19]. It has been shown that the D value obtained from IVIM exhibited better performance than conventional DWI and may serve as a potential imaging biomarker for cancer invasion and cell proliferation [19,20]. In this study, the characteristics of EHCC with different Ki-67 expression were evaluated by comparison in D*, f and D values calculated by an IVIM-DWI double-index model, and ADC values calculated by the single index model.

### 4.1. Correlations of D and ADC values with Ki-67 expression

The proliferation activity of tumor cells is closely related to biological behavior [21,22]. Rapid tumor growth increases the likelihood of

**Table 1**
Comparison in ADC, D, f and D* values of EHCC with different Ki-67 expression.

| Ki-67 expression grouping (n) | ADC ($\times 10^{-3}$ mm$^2$/s) | D ($\times 10^{-3}$ mm$^2$/s) | $f$ (%) | D* ($\times 10^{-3}$ mm$^2$/s) |
|---|---|---|---|---|
| Group I (5) | 1.35 ± 0.21 | 1.30 ± 0.16 | 38.26 ± 9.15 | 6.41 ± 2.31 |
| Group II (13) | 1.24 ± 0.18 | 1.18 ± 0.14 | 32.09 ± 8.59 | 6.04 ± 2.05 |
| Group III (17) | 1.10 ± 0.15 | 1.05 ± 0.14 | 28.71 ± 7.93 | 5.81 ± 2.21 |
| Group IV (7) | 0.96 ± 0.12 | 0.87 ± 0.11 | 22.45 ± 7.23 | 5.47 ± 1.98 |
| F | 24.37 | 39.23 | 10.83 | 1.71 |
| P | 0.000 | 0.000 | 0.000 | 0.190 |
| *r* | −0.607 | −0.795 | −0.531 | −0.213 |
| P | 0.000 | 0.000 | 0.000 | 0.089 |

infiltration and metastasis of tumor cells. It has been reported that the Ki-67 index in EHCC cells is significantly higher than that in the surrounding tissues [21,22]. The index is closed related to the degree of EHCC differentiation, lymphatic metastasis, and clinical stage, which can be used as an important index for judging EHCC prognosis [21,22].

With elevated Ki-67 expression, proliferation of tumor cells becomes activated, leading to an abnormally dense arrangement of cells, and causing a reduction in the extracellular space. In addition, the cell nucleus enlarges, increasing the ratio of nucleus to cytoplasm, and decreasing the intracellular space, resulting in relatively compressed motion space for water molecules, and more significant limitation in free diffusion [23,24]. The ADC and D values representing diffusion are reduced accordingly. Our results showed that with increasing Ki-67 expression, the ADC and D values of each group decreased, leading to a significant negative correlation ($P = 0.000$). The correlation of D with Ki-67 expression was the highest. The possible reason is that D eliminates the influence of microcirculation blood flow perfusion on the diffusion coefficient in traditional DWI, which more accurately reflects the perfusion information of water molecules in the tissues and organs, as well as the Ki-67 expression in tumor. Thus, D can be used as an index predicting Ki-67 expression in extrahepatic cholangiocarcinoma, which is helpful to evaluate the prognosis of cancer patients.

Correlations of IVIM related perfusion parameters (f, D*) with Ki-67 expression.

The D value in the IVIM double-index model mainly reflects the constitution of tissues, and the f and D*values mainly reflect neovascularization and permeability of tissues. According to the literature, there was a moderate correlation between f and Ki-67 expression, and f can be used for quantitative prediction of Ki-67 expression [25,26]. In theory, faster tumor cell proliferation leads to more abundant tumor vessels. The D* and f values mainly reflect the blood capillary density and microcirculation perfusion in tumor tissues, which would be expected to increase with increasing proliferation. However, our study indicated that f value had a moderately negative correlation with Ki-67 expression, and the correlation was poorer than that of ADC and D values. The main components of EHCC include viable tumor cells, coagulative necrosis, fibrous tissues, and mucoprotein, characteristic of a hypovascular tumor. With increasing Ki-67 expression, the atypia of tumor cells is more significant. The normal tissues suffer from infiltration and damage, the necrotic elements are increased, and the microcirculation is gradually reduced [27–30], such that the perfusion fraction, f, is reduced accordingly. F reflects the poor blood supply of EHCC, which is in line with previous studies [27–30]. It has been reported that EHCC shows low perfusion on perfusion maps, and the lower perfusion value suggests a lower degree of tumor differentiation. The low perfusion value may be related to angiosclerosis, tumor invading vessels, and tumor necrosis caused by intimal hyperplasia of arterioles adjacent to the tumor. The correlation of f with Ki-67 expression is relatively low. The possible reason is that Ki-67 expression reflects cell proliferation rather than angiogenesis. The differences in D* among groups with different Ki-67 expression were not statistically significant. The possible reason is that the signal-to-noise ratio of D* on pseudo-color imaging is low, and the individual differences of D* are large, leading to increased deviation when measuring.

So far, the application of IVIM-DWI in EHCC still has some problems. Respiratory trigger technique is used to reduce respiratory motion artifact. Parallel acquisition technique, shortened TE, and local replacement of the saturation zone have been used to effectively reduce artifact and improve image quality. Although D had a significant correlation with Ki-67 expression, the data of the four groups had overlap to a certain degree. The diagnostic efficiency still needs further exploration.

Above all, ADC, D and f values of IVIM negatively correlate with the Ki-67 expression level of EHCC. The correlation and diagnostic efficiency of D was the highest and those of f value were the lowest. Thus, IVIM-DWI applied in EHCC is superior to the single-index model. D value can be used to judge proliferation degree of extrahepatic cholangiocarcinoma, quantitatively evaluate the prognosis, and provide an important reference to guide individualized treatment.

## Acknowledgement

This study was supported by the National Natural Science Foundation of China (No.81271629) and Wuxi Medical Leading Talent and Innovation Team(No. CXTD002).

## References

[1] Razumilava N, Gores GJ. Cholangiocarcinoma. Lancet 2014;383(9935):2168–79.
[2] Friman S. Cholangiocarcinoma-current treatment options. Scand J Surg 2011;100(1):30–4.
[3] Matsuo K, Rocha FG, Ito K, et al. The Blumgart preoperative staging system for hilar cholangiocarcinoma: analysis of resectability and outcomes in 380 patients. J Am Coll Surg 2012;215(3):343–55.
[4] Inwald EC, Klinkhammer-Schalke M, Hofstädter F, et al. Ki-67 is a prognostic parameter in breast cancer patients: results of a large population-based cohort of a cancer registry. Breast Cancer Res Treat 2013;139(2):539–52.
[5] Aydin H, Guner B, Esen Bostanci I, et al. Is there any relationship between adc values of diffusion-weighted imaging and the histopathological prognostic factors of invasive ductal carcinoma? Br J Radiol 2018;91(1084):20170705.
[6] Surov A, Meyer HJ, Höhn AK, et al. Correlations between intravoxel incoherent motion (IVIM) parameters and histological findings in rectal cancer: preliminary results. Oncotarget 2017;8(13):21974–83.
[7] Wen S, Zhou W, Li CM, et al. Ki-67 as a prognostic marker in early-stage non-small cell lung cancer in Asian patients: a meta-analysis of published studies involving 32 studies. BMC Cancer 2015;15:520.
[8] Surov A, Meyer HJ, Wienke A. Associations between apparent diffusion coefficient (ADC) and KI 67 in different tumors: a meta-analysis. Part 1: ADCmean. Oncotarget 2017;8(43):75434–44.
[9] Surov A, Meyer HJ, Wienke A. Correlation between apparent diffusion coefficient (ADC) and cellularity is different in several tumors: a meta-analysis. Oncotarget 2017;8(35):59492–9.
[10] Surov A, Meyer HJ, Wienke A. Can imaging parameters provide information regarding histopathology in head and neck squamous cell carcinoma? A meta-analysis. Transl Oncol 2018;11(2):498–503.
[11] Kobayashi S, Koga F, Kajino K, et al. Apparent diffusion coefficient value reflects invasive and proliferative potential of bladder cancer. J Magn Reson Imaging 2014;39(1):172–8.
[12] Driessen JP, Caldas-Magalhaes J, Janssen LM, et al. Diffusion-weighted MR imaging in laryngeal and hypopharyngeal carcinoma: association between apparent diffusion coefficient and histologic findings. Radiology 2014;272(2):456–63.
[13] Surov A, Gottschling S, Mawrin C, et al. Diffusion weighted imaging in meningioma:

predictiong of tumor grade and association with histopathological parameters. Transl Oncol 2015;8(6):517–23.
[14] Hambrock T, Somford DM, Huisman HJ, et al. Relationship between apparent diffusion coefficients at 3.0-T MR imaging and Gleason grade in peripheral zone prostate cancer. Radiology 2011;259(2):453–61.
[15] Iima M, Le Bihan D, Okumura R, et al. Apparent diffusion coefficient as an MR imaging biomarker of low-risk ductal carcinoma in situ: a pilot study. Radiology 2011;260(2):364–72.
[16] Le Bihan D, Breton E, Lallemand D, et al. Separation of diffusion and perfusion in intravoxel incoherent motion MR imaging. Radiology 1988;168(2):497–505.
[17] Hu XX, Yang ZX, Liang HY, et al. Whole-tumor MRI histogram analyses of hepatocellular carcinoma: correlations with Ki-67 labeling index. J Magn Reson Imaging 2017;46(2):383–92.
[18] Kim Y, Ko K, Kim D, et al. Intravoxel incoherent motion diffusion-weighted MR imaging of breast cancer: association with histopathological features and subtypes. Br J Radiol 2016;89(1063):20160140.
[19] Yiping L, Kawai S, Jianbo W, et al. Evaluation parameters between intra-voxel incoherent motion and diffusion-weighted imaging in grading and differentiating histological subtypes of meningioma: a prospective pilot study. J Neurol Sci 2017;372(1):60–9.
[20] Wang F, Wu LM, Hua XL, et al. Intravoxel incoherent motion diffusion-weighted imaging in assessing bladder cancer invasiveness and cell proliferation. J Magn Reson Imaging 2018;47(4):1054–60.
[21] Zhao W, Zhang B, Guo X, et al. Expression of Ki-67, Bax and p73 in patients with hilar cholangiocarcinoma. Cancer Biomark 2014;14(4):197–202.
[22] Aloysius MM, Hewavisenthi SJ, Bates TE, et al. Predictive value of tumor proliferative indices in periampullary cancers: Ki-67, mitotic activity index (MI) and volume corrected mitotic index (M/V) using tissue microarrays. World J Surg 2010;34(9):2115–21.
[23] Zhang YD, Wang Q, Wu CJ, et al. The histogram analysis of diffusion-weighted intravoxel incoherent motion (IVIM) imaging for differentiating the Gleason grade of prostate cancer. Eur Radiol 2015;25(4):994–1004.
[24] Woo S, Lee JM, Yoon JH, et al. Intravoxel incoherent motion diffusion -weighted MR imaging of hepatocellular carcinoma: correlation with enhancement degree and histologic grade. Radiology 2014;270(3):758–67.
[25] Xiao Z, Zhong Y, Tang Z, et al. Standard diffusion-weighted, diffusion kurtosis and intravoxel incoherent motion MR imaging of sinonasal malignancies: correlations with Ki-67 proliferation status. Eur Radiol 2018;28(7):2923–33.
[26] Wang CC, Dong HB, Ding F, et al. Quantitative evaluation of intravoxel incoherent motion diffusion-weighted imaging and three-dimensional arterial spin labeling in Ki-67 labeling index and grading of brain gliomas. Zhonghua Yi Xue Za Zhi 2019;99(5):338–42.
[27] Razumilava N, Gores GJ. Classification, diagnosis, and management of cholangiocarcinoma. Clin Gastroenterol Hepatol 2013;11(1):13–21.
[28] Rizvi S, Gores GJ. Pathogenesis, diagnosis, and management of cholangiocarcinoma. Gastroenterology 2013;145(6):1215–29.
[29] Rizvi S, Borad MJ, Patel T, et al. Cholangiocarcinoma: molecular pathways and therapeutic opportunities. Semin Liver Dis 2014;34(4):456–64.
[30] Yao D, Kunam VK, Li X. A review of the clinical diagnosis and therapy of cholangiocarcinoma. J Int Med Res 2014;42(1):3–16.